Understanding the contact resistance in an ACF bonding

Helge Kristiansen
Conpart AS
Dragonveien 54
2013 Skjetten
helge@conpart.no

Giang M..Nghiem
Dept. of Microsystems
University of South-Eastern Norway
Vestfold, Norway
Giang.Nghiem@usn.no

Molly Bazilchuk
Ducky AS
Kjøpmannsgata 51, 7011 Trondheim
molly@ducky.eco

Knut E. Aasmundtveit
Dept. of Microsystems
University of South-Eastern Norway
Vestfold, Norway
kaa@usn.no,
ORCID: 0000-0001-9003-1916

***Abstract*— Anisotropic Conductive Film (ACF) bonding, the technique of choice for display interconnects, allows very fine pitch interconnect at a moderate process temperature, typically at the expense of a non-negligible interconnect resistance. Modern ACFs have conducting particles in a thin layer of high-viscosity adhesive. This allows even finer pitch but comes at the risk of high interconnect resistance due to trapped adhesive between pad and conductive particle. Conductive particles with spikes are designed to penetrate such a trapped adhesive layer.**

In this paper, we compare spiky conductive particles with the traditional, spherical, ones. We measure interconnect resistance of individual particles in a nano-indentation test setup, as well as the interconnect resistance of ACF bonding using the two different particles, in daisy-chain measurements.

Interconnect resistance of individual spiky particles is more than an order of magnitude higher than the one for spherical particles. However, when mixed in an adhesive and used for ACF bonding, the interconnect resistance of ACF with spiky particles is somewhat lower than that of the ACF with spherical particles. The interconnect resistance of ACF with spherical particles is two orders of magnitude higher than that of the individual particles, whereas the interconnect resistance of ACF with spiky particles is comparable to the individual-particle resistance.

We conclude that trapped adhesive is a major concern for fine-pitch ACF bonding, and that the use of spiky conductive particles has the potential to overcome these challenges.

Keywords—anisotropic conductive adhesive, ACF bonding, metal-coated polymer spheres (MPS), fine-pitch bonding, trapped adhesive

I. INTRODUCTION

Anisotropic Conductive Film (ACF) is today the standard interconnect technology for display applications. The technology allows a very fine pitch interconnect and a moderate temperature during the assembly process. To improve the fine pitch capabilities of the technology, double layer ACF has been introduced, where the particles are confined to a thin layer of adhesive with extra high viscosity. The aim is to increase the area density of conducting particles and at the same time avoid uncontrolled flow of the conductive particles during bonding.

The Achilles heel of the technology, is that the contact resistance is a concern since advanced display technologies require higher current densities than the traditional ones. Contact resistance has been addressed experimentally and by modelling. ACF interconnect resistance is typically higher than what is predicted by a simplified model of a metal-coated polymer particle compressed between two contact pads [1][2][3], implying that additional factors play a role. The contact resistance depends on several factors, the main are:

- Number of particles and their state of compression
- Effective conductivity of particle metallisation
- Effective contact area (given by the alignment accuracy)
- Particle deformation and contact topography
- Presence of particle insulation
- Trapped adhesive between particle and the respective contacts

Experimental measurements of contact resistance typically include a number of uncertainties:

- Bump and pad design makes the effective contact area (and hence number of particles) strongly dependent on bonding alignment
- Unknown or highly variable particle deformation due to the roughness of the bump surface and lack of bond planarity

Previous studies [2][3][4] have indicated that trapped adhesive film at the contact area is a major cause for the interconnect resistance being higher than expected, but a thorough experimental investigation is lacking. The resistance of single particles (without adhesive present) has been measured by electromechanical testing as a function of deformation, adding new insight [5]. In this paper, we compared such single-particle resistance (as measured in electromechanical testing) with ACF interconnect resistance (as measured for daisy chains in ACF bonded test vehicles) for two different metal-coated polymer particles.

This work is funded by the Norwegian Research Council through the project "Novel Particle for Display Interconnect", project number 228453 and through the Norwegian Micro- and Nano-Fabrication Facility (NorFab, project number: 295864).

II. Experimental

A. Design and manufacturing of test circuits

The test circuits were based on a silicon die measuring 10 mm x 2 mm, mounted onto a glass substrate. The silicon die has Al wiring, Si_3N_4 passivation and 10 µm high electro-plated gold bumps. The test dies were fabricated by Taiwan Semiconductor Manufacturing Company (TSMC). The test vehicle included 5 daisy chains all containing 406 connections, each chain with different bump size. The daisy chains were divided into 12 segments of different lengths and was measured using a probe card. Total resistance in the measurement system including probes and their contact to the probe pads was below 10Ω. This is less than 5% of the resistance measured in the segments and is therefore neglected. The size of the gold bumps in the different daisy chains are 30x10, 35x10, 40x10, 40x15 and 60x15µm^2 respectively. To minimize the variation of the bump gap, one of the test chip wafers were planarized using a DAS 8920 surface planar at Disco in Taiwan. The surface topography of the test chip bumps was examined by a Wyko NT9100 interferometer.

The glass substrate was made by Industrial Technology Research Institute (ITRI) using Ti/Al/Ti metallization stack covered with ITO using a Ti/Al/Ti metallisation stack covered with an ITO layer. The substantial over-sized contact pads (80x90µm^2) on the glass substrate allows some degree of misalignment without changing on the effective contact area. For more information on the test circuits, we refer to [6].

B. Conductive particles and ACF

For this experiment two different ACFs based on an epoxy system, were prepared by Hitachi Chemicals, specified in Table 1. The total adhesive thickness was 15 µm, with all the particles confined in a 4 µm thick layer of a higher viscosity resin.

Two different types of conductive particles were used in this experiment, both based on the same acrylic polymer core of 3.0 µm. One was plated with "Spiky Ni" by Hitachi Chemicals, the other with a traditional Ni-Au coating plated by Conpart. The surface roughness of the nickel coating of the spiky particle is of the order of hundred nanometres. Additionally, a fraction of the area of small (≈200 nm) polymer particles is added to the surface to improve the dispersion in the adhesive and avoid particle to particle contact, see Figure 1.

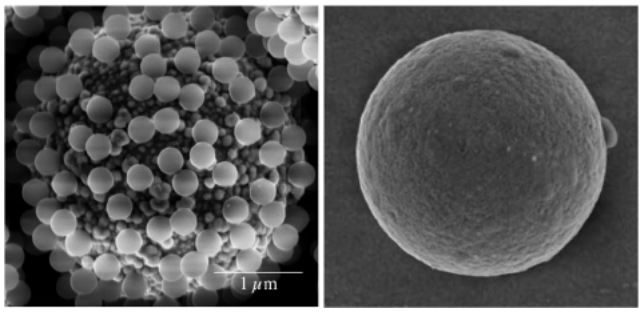

(a) (b)

Fig. 1. a) Polymer core particle with spiky Ni plating. The surface is covered with small (≈ 200 nm) polymer particles. b) Polymer core particles with Ni-Au plating.

TABLE I. ACF system specification

ACF system	Type of conductive particle
ACF 1	Smooth Ni-Au
ACF 2	Spiky Ni
ACF Components	
Adhesive	Acrylic
Ni-Au	3.0 µm Acrylic core, coating 100nm Ni/20nm Au
Spiky Ni	3.0 µm Acrylic core, coating 150nm Ni
Particle density	16 -18,000 particles per mm^2

C. Nanoidentation

The electrical properties of the two types of conductive particles have been measured using electrical nanoindentation, see Figure 2. The particle under test is placed between an indenter tip made of platinum-iridium and a gold coated silicon substrate, surrounded by normal air. During the test, the particle is compressed by a load increasing with 1.2 mN/s for 5 s, a hold stage of 2 s followed by unloading with the same rate. The total resistance from tip to substrate as well as the deformation is measured every 50 ms, as the indenter-tip is compressing the particle. A fixed resistance range of 100 Ω was chosen to minimize the time of measurement. In this way, the electrical performance of individual conductive particles was tested as function of mechanical deformation in a way mimicking the ACF bonding process, but crucially without the presence of an adhesive resin. This method is described in detail in [5].

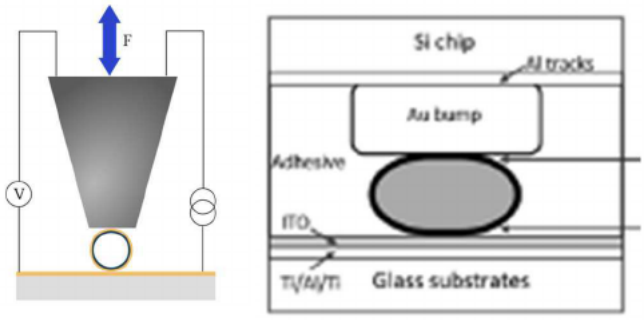

Fig. 2. Comparing Nano-indentation and ACF bonding

D. Assembly and testing of test circuits

The test circuits were assembled at Hitachi Chemicals research center. ACF was laminated to the glass / ITO substrate at 90ºC for 3 seconds. After removing the carrier film, the test chip was aligned and pre-bonded to the glass substrate. The test vehicles were then moved to the bonding unit where the actual bonding took place at 150ºC for 5 seconds. A thin PTFE film was inserted between the component and the bonding head.

Each component bonded to the patterned substrate was inspected using differential interference contrast (DIC) microscopy which makes it possible to observe the imprint from the particle on the pad from below, through the pad metallisation. The number of conductive particles were counted for several specified pads. A few components were also bonded to a non-patterned area of the glass that made it possible to inspect with traditional microscopy.

TABLE II. MEASURED BUMP AREA [μm²] FOR THE DIFFERENT DAISY CHAINS

Daisy chain	900	600	400	350	300
	Avg.	Avg.	Avg.	Avg.	Avg.
Planarized bump	920	570	330	290	250
Un-planarized bump	810	510	315	270	225

TABLE III. AVERAGE NUMBER OF CAPTURED PARTICLES AT DIFFERENT BUMP SIZES FOR DIFFERENT ACFS

	Number of particles									
Type of ACF	900μm²		600μm²		400μm²		350μm²		300μm²	
	Avg.	Std	Avg.	Std	Avg.	Std	Avg.	Std	Avg.	Std
ACF 1	17	3	11	3	7	2	6	2	6	2
ACF 2	15	3	9	2	6	2	5	2	4	1

Note- The statistics for ACF 1 and ACF 2 was measured on planarized IC samples.

The electrical resistance of the daisy chains was measured using 4-point measurement using a probe card. A Keithley 3706 System Switch / Multimeter was used for the measurements.

After electrical testing, some of the components were moulded in epoxy and cross-sectioned by mechanical grinding and polishing. The polishing process was consistently conducted in the direction from ITO toward Au bump and at a very slow speed to minimize any metal smearing. This also allowed for the measurement of the bond gap between bump and pad for the different bump sizes and bonding pressures.

III. RESULTS AND DISCUSSION

A. Planarization

Figure 3 shows the typical topography of the small (300 μm²) and large (900 μm²) bumps. Table 2 shows test chip bump area before and after planarization process. The variation in bump height between different bump sizes is less than 0.1μm, both for the planarized and un-planarized test chip. The bump sidewalls are slightly inclined, and hence the planarization of the bumps slightly increases the bump area, see Table 2. The planarization process also seems to create a slight smearing of the soft gold bump, see Figure 4. The bump area for the planarized bumps is 5 to 15% larger than for the un-planarized bumps.

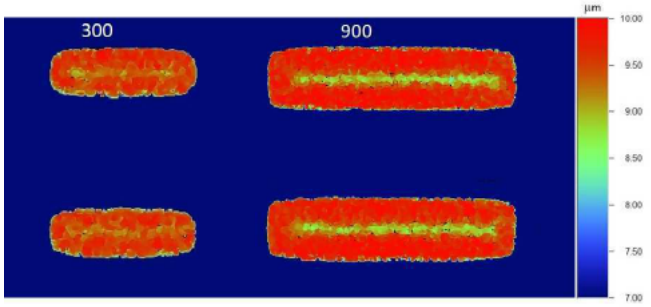

Fig. 3. Interferometry measurement of un-planarized bump surface at sizes 300 and 900 μm ²

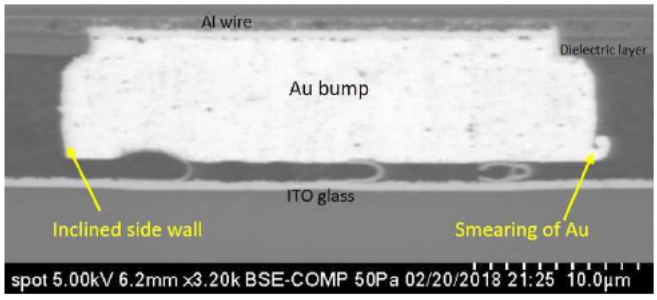

Fig. 4. Cross-section of planarized bump for a nominal bump size of 350μm²

B. Particle distributions

Table 3 shows the number of conducting particles captured between the bump and ITO electrodes is slightly higher (~10-20%) for ACF 1 than for ACF 2. All measurements in Table 3 gives a particle density within the range specified for the ACFs (Table 1), showing that there is no significant flow of particles during ACF bonding.

C. Mechanical testing of conductive particles

Ten particles of each type were tested in the nano-indenter. Typical mechanical results are shown in Figure 5. There is a significant difference in the compression curve, "shifting" the Spiky Ni particles towards a larger "deformation" in the very early stage of the test. Within 50 ms the position of the indenter tip suddenly moves more than 300 nm, that is reflected in the rest of the measurement curve. This sudden displacement is typically described as a "pop-in". This is probably caused by a displacement of the tiny polymer particles on the nickel surface.

Further increasing the deformation of the particles, the nickel layer will fracture, typically around 15-20% particle deformation [7], This is observed in the measurements causing a sudden "pop-in". On the Ni-Au and Spiky Ni coated particles this is observed in the region of 400 to 550nm and 1000-1200nm respectively.

In this test, we observed fracture of the polymer core in 3 of the 10 NiAu particles and 6 of the 10 Spiky Ni particles.

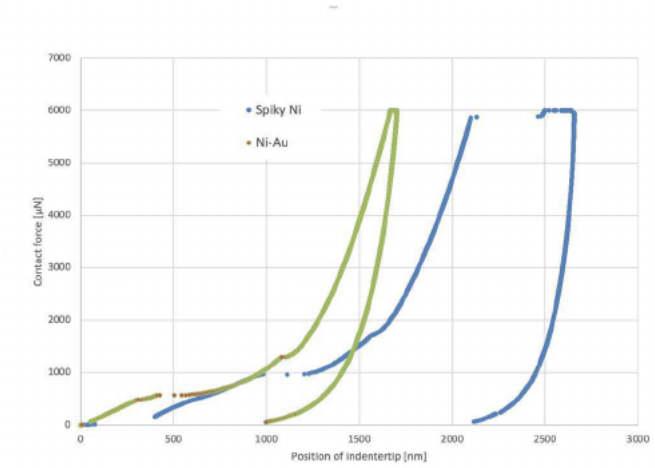

Fig. 5. Typical mechanical behaviour of the Spiky Ni particles (blue) and Ni-Au coated particles (green).

D. Electrical testing

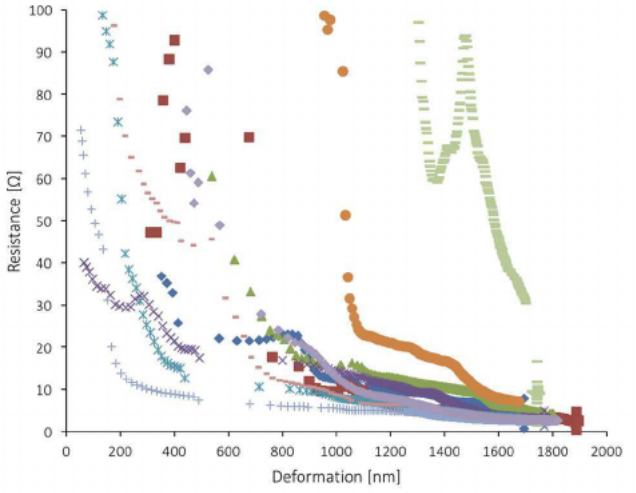

a)

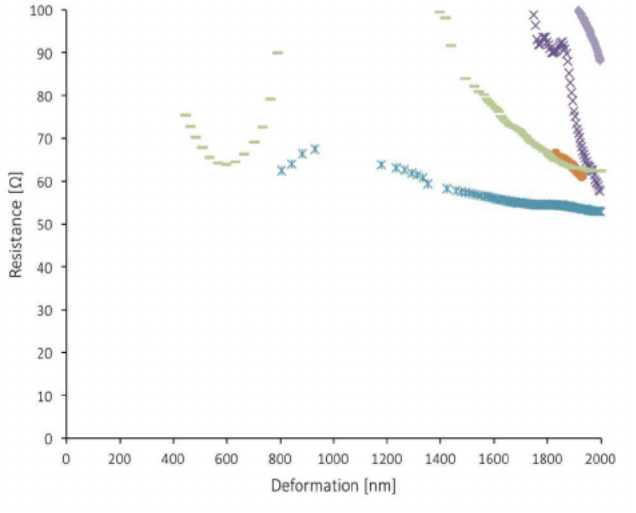

b)

Fig. 6. The resistance-deformation characteristics of individual Ni-Au particles on an Au-coated silicon substrate (a) and spiky Ni particles on same substrate (b). Each curve represents a single particle.

The electrical results from the nano-indentation testing shows a significant difference in the behaviour of the two different particles, see figure 6. The NiAu particles shows a large variation in resistance at small deformations but converging towards a value slightly below 3Ω as the deformation reaches 50%. This value is an order of magnitude higher than what would be expected from a first order theoretical model. The contact resistance of the Spiky Ni particles is even much higher, in fact, only a few of these reach a contact resistance below 100Ω before the polymer core fractured.

E. Deformation and planarization

Due to the test chip design, we observed a significantly thicker bond-line at the side with the large bond pads compared to the side of the small bond pads. This appeared consistently throughout all the components, irrespectively of the type of ACF and bonding pressure. This significantly complicated the interpretation of the results.

F. ACF bonding

The resistance of all the daisy chain segments was measured and the average contact resistance was calculated by dividing with the number of contacts in the segment. A typical contact resistance for the individual particle is then estimated by multiplying the contact resistance by the average number of particles for the given bump size.

In Figure 7 we present results from four different components, including the two different types of particles as well as planarized (P) and non-planarized (NP) bumps, all bonded with a force of 40N. All the results are displayed as the contact resistance per particle. It is clear from the results that the smaller pads provide lower contact resistance per particle. This is due to the asymmetry of the component which causes a tilt towards the smaller pads, and hence increased particle deformation.

Despite a much higher resistance in the nano-indenter test, the spiky Ni particles obtained a lower contact resistance in the ACF test than the NiAu particles.

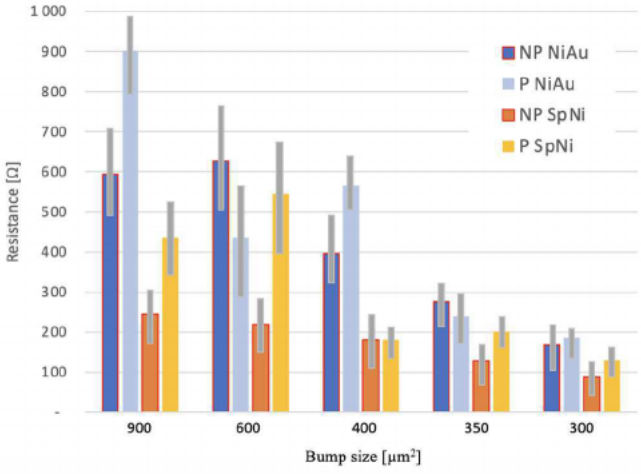

Fig. 7. Resistance per conductive particle, comparing NiAu and Spiky Ni particles as well as planarized and non-planarized bumps. All results are for a bonding force of 40N.

In Figure 8 we have compared the contact resistance for the two different particles in the nano indenter and in ACF bonding as a function of bond gap. We see that in the ACF test the NiAu particles the contact resistance was approximately

two orders of magnitudes higher than in the nano-indenter test. This large difference in contact resistance for the Ni-Au particles can be explained by the fact that during the bonding, the adhesive film between the conducting particles, and the bump and the pad respectively, needs to be squeezed out to provide a good electrical contact. With the smooth surface of the NiAu particles there seems to remain a thin layer of the adhesive in one or both of these contact areas. This problem has been further increased by the introduction of the doubler layer adhesive where the viscosity of the particle layer has been increased to minimize the flow of the particles.

On the other hand, for the spiky Ni particles there is no big difference in the contact resistance measured by the two different test methods. This is likely because the spiky surface more easily penetrates the adhesive layer. Additionally, the thicker nickel layer increased the stiffness of the spiky particles.

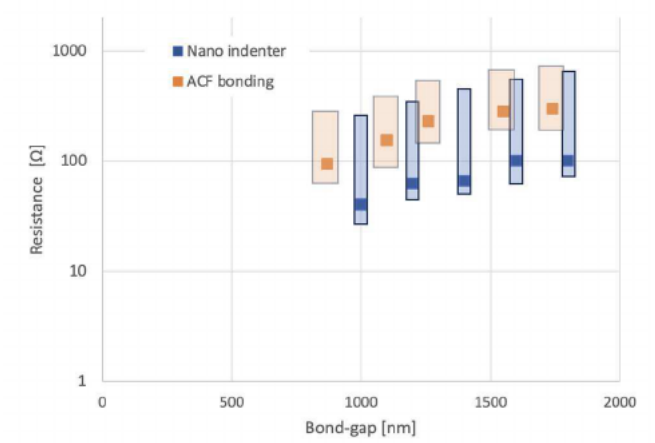

a)

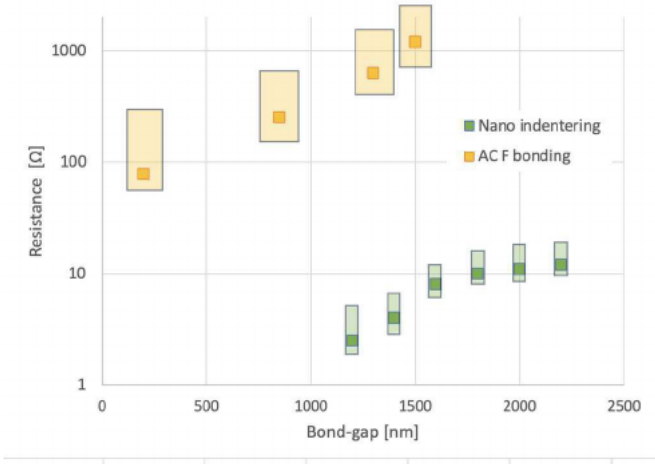

[8]

b)

Fig. 8. : Comparing the contact resistance measured in nano-indentation and in an ACF bonding as a function of bond gap for, a) spiky Ni particles and b) Ni-Au coated particles. The bumps on both components have been planarized.

IV. Conclusion

ACF bonding allows very fine pitch interconnects, but comes at the expense of higher interconnect resistance. The use of double layer adhesive with high viscosity of the layer containing particles risks increasing the interconnect resistance due to adhesive trapped at the interfaces.

We demonstrate in this paper that traditional, spherical conductive particles will indeed face this challenge, as the interconnect resistance can increase two orders of magnitude compared to the individual particles. Using spiky particles, a lower ACF bonding contact resistance is achieved, due to puncturing of the adhesive layer.

Acknowledgment *(Heading 5)*

Takashi Nakazawa, Kazuya Matsuda and Masaru Tanaka, at Hitachi Chemical for the manufacturing of the ACF and providing the bonding of the test samples. Grand Cheng and Josh Chen at Disco Taiwan for providing the planarization of the gold bumps. The Norwegian Research Council for funding of the project “Novel Particle for Display Interconnect”, project number 228453 and for and the Norwegian Micro- and Nano-Fabrication Facility (NorFab, project number: 295864).

References

[1] M. Chin, K. A. Iyer, and S. J. Hu, “Prediction of electrical contact resistance for anisotropic conductive adhesive assemblies,” *IEEE Trans. Components Packag. Technol.*, vol. 27, no. 2, pp. 317–326, 2004.

[2] J. H. Constable, “Analysis of the Constriction Resistance in an ACF Bond,” *IEEE Trans. Components Packag. Technol.*, vol. 29, no. 3, pp. 494–501, 2006.

[3] C. N. Oguibe, S. H. Mannan, D. C. Whalley, and D. J. Williams, “Conduction mechanisms in anisotropic conducting adhesive assembly,” in *Proceedings. The First IEEE International Symposium on Polymeric Electronics Packaging, PEP ’97 (Cat. No.97TH8268)*, 1997, pp. 249–258.

[4] R. L. Jackson and L. Kogut, “Electrical Contact Resistance Theory for Anisotropic Conductive Films Considering Electron Tunneling and Particle Flattening,” *IEEE Transactions on Components and Packaging Technologies*, vol. 30, no. 1. pp. 59–66, 2007.

[5] M. Bazilchuk, S. R. Pettersen, H. Kristiansen, Z. Zhang, and J. He, “Electromechanical characterization of individual micron-sized metal coated polymer particles”, Journal of Applied Physics 119, 245102 (2016); doi: 10.1063/1.4954218

[6] G. M. Nghiem, K. E. Aasmundtveit, H. Kristiansen and M. Bazilchuk, "Anisotropic Conductive Film (ACF) bonding: effect of interfaces on contact resistance," 2018 7th Electronic System-Integration Technology Conference (ESTC), 2018, pp. 1-5, doi: 10.1109/ESTC.2018.8546414.

[7] Fracture of micrometre-sized Ni/Au coated polymer particles, He J Y, Helland T, Zhang Z L, Kristiansen H., Journal of Physics D: Applied Physics 2009; 42(8): 085405 (5pp)